

Supporting Information

**Revealing the annealing effects of annealing on Li-ion mobility in the $\text{Li}_6\text{PS}_5\text{Br}$ solid electrolyte
synthesized by a mechanical milling route**

Chuang Yu^a, Swapna Ganapathy^a, Ernst R.H. van Eck^b, Lambert van Eijck^a, Shibabrata Basak^c,
Yanyan Liu^d, Long Zhang^d, Henny W. Zandbergen^c, Marnix Wagemaker^{a,*}

^a Department of Radiation Science and Technology, Delft University of Technology, Mekelweg
15, 2629JB Delft, The Netherlands

^b Institute for Molecules and Materials, Radboud University Nijmegen, Heyendaalseweg 135,
6525 AJ Nijmegen, The Netherlands

^c Kavli Institute of Nanoscience Delft, Department of Quantum Nanoscience, Delft University of
Technology, Lorentzweg 1, 2628 CJ Delft, The Netherlands

^d State Key Laboratory of Metastable, Materials Science and Technology, Yanshan University,
Qinhuangdao, Hebei 066004, China

Table S1. Room temperature X-ray diffraction patterns including Rietveld refinement of the (a) $\text{Li}_6\text{PS}_5\text{Br}$, (b) AN- $\text{Li}_6\text{PS}_5\text{Br}$, (c) and AN-BM- $\text{Li}_6\text{PS}_5\text{Br}$ materials.

	Atom	Fractional coordinates			Wyckoff	Occupancy	U _{iso}
		X	Y	z			(Å ²)
	Li	0.174(5)	0.174(5)	0.029(0)	48h	0.47(3)	0.172(7)
BM- Li ₆ PS ₅ Br	P	0.5	0.5	0.5	4b	1.0	0.080(5)
F-43m	S(0)	0.617(3)	0.617(3)	0.617(3)	16e	1.0	0.074(3)
a=9.941(7) Å	S(1)	0.0	0.0	0.0	4c	0.52(5)	0.080(6)
	Br(1)	0.0	0.0	0.0	4c	0.47(5)	0.025(3)
	S(2)	0.25	0.25	0.25	4a	0.56(3)	0.065(6)
	Br(2)	0.25	0.25	0.25	4a	0.43(7)	0.055(8)

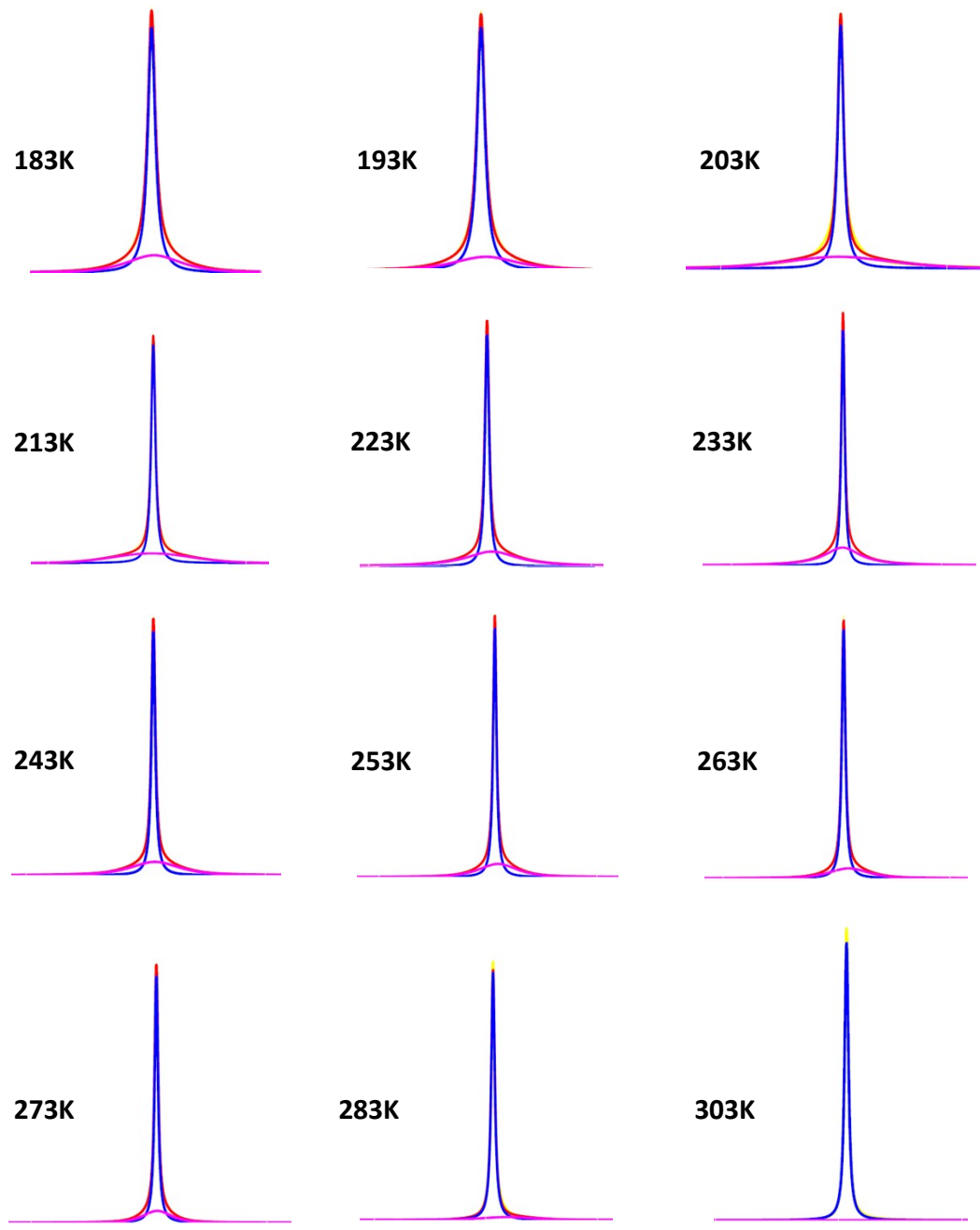


Figure S1. The line shape of $\text{Li}_6\text{PS}_5\text{Br}$ measured from 183 to 303 K, which are fit as a sum of Gaussian (broad) and Lorentzian component (narrow) associated with slow and fast lithium ion motilities. Here, the fit results of AN- $\text{Li}_6\text{PS}_5\text{Br}$ is shown as an example.

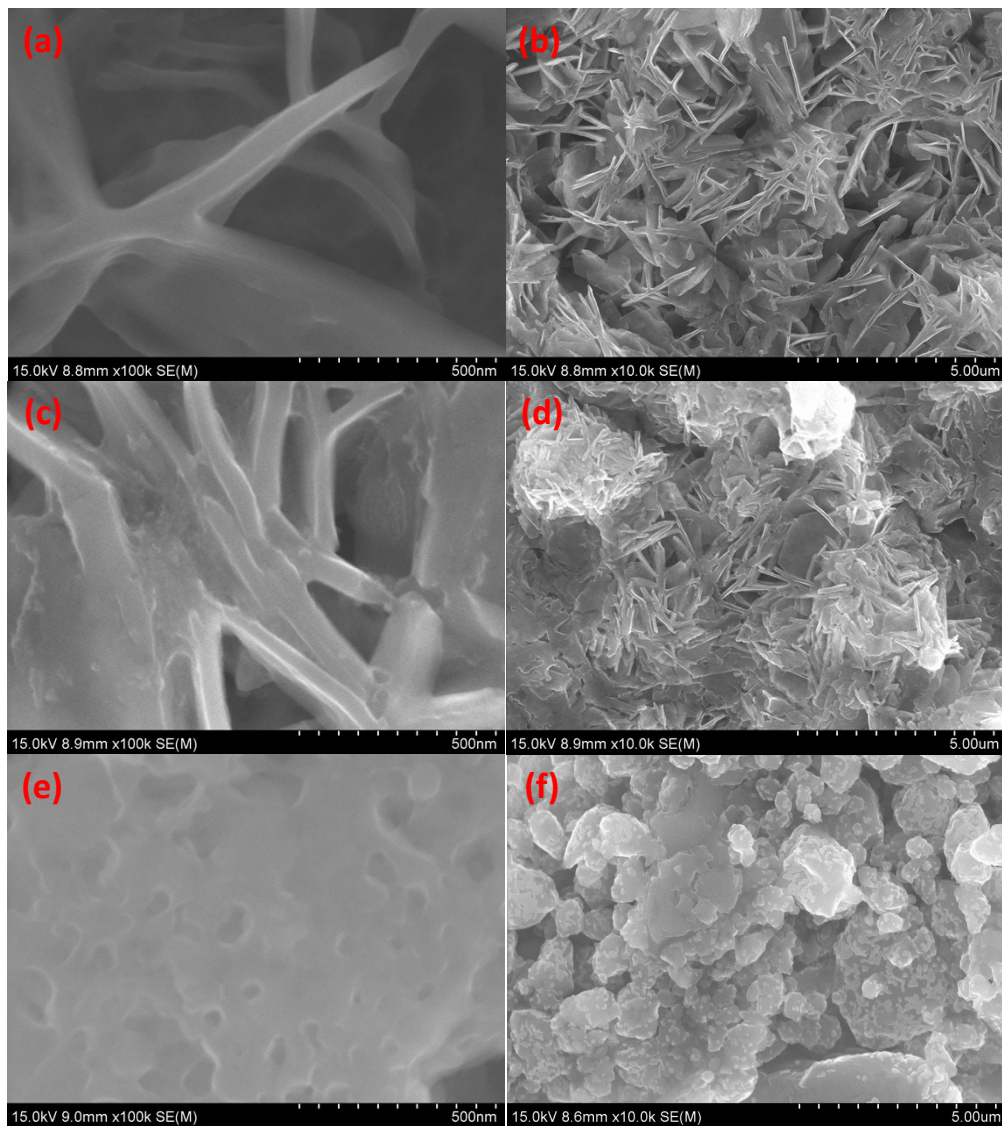


Figure S2. SEM images of the samples (a-b) $\text{Li}_6\text{PS}_5\text{Br}$, (c-d) AN- $\text{Li}_6\text{PS}_5\text{Br}$, and (e-f) AN-BM- $\text{Li}_6\text{PS}_5\text{Br}$.

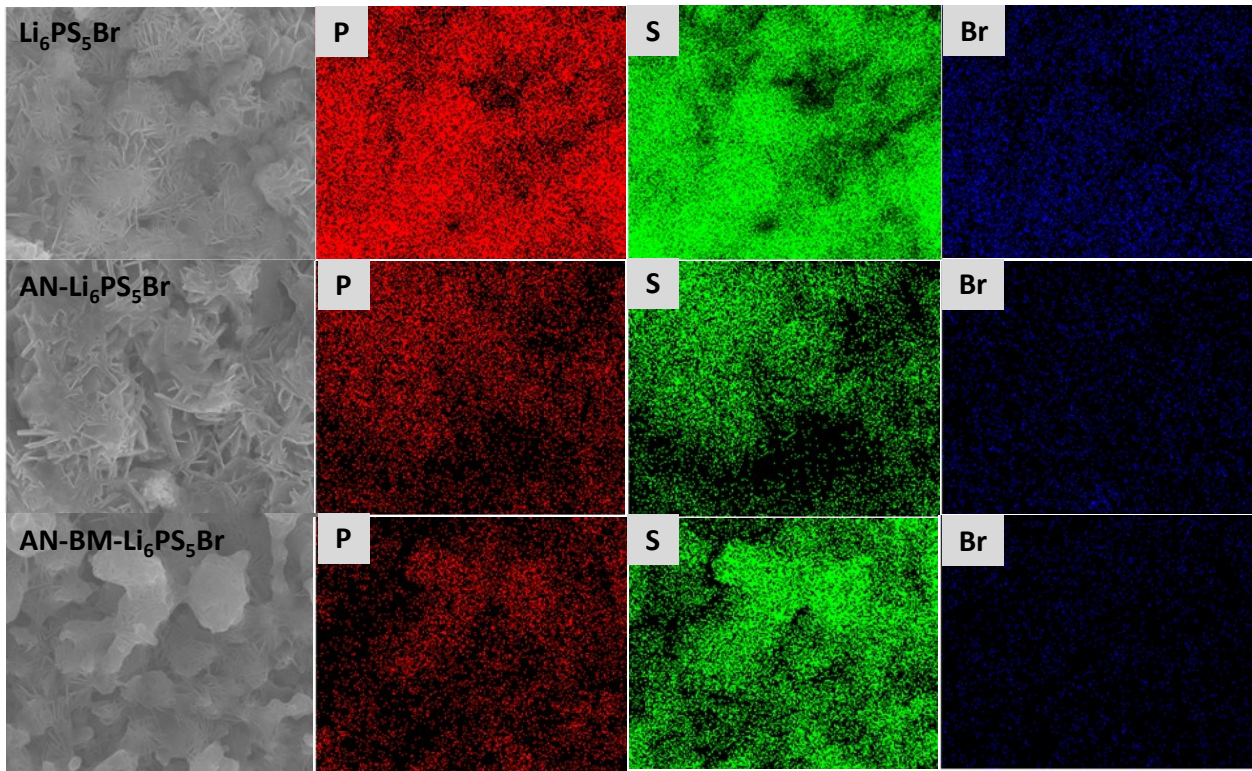


Figure S3. The EDS mapping of the samples (a-b) $\text{Li}_6\text{PS}_5\text{Br}$, (c-d) $\text{AN-Li}_6\text{PS}_5\text{Br}$, and (e-f) $\text{AN-BM-Li}_6\text{PS}_5\text{Br}$.

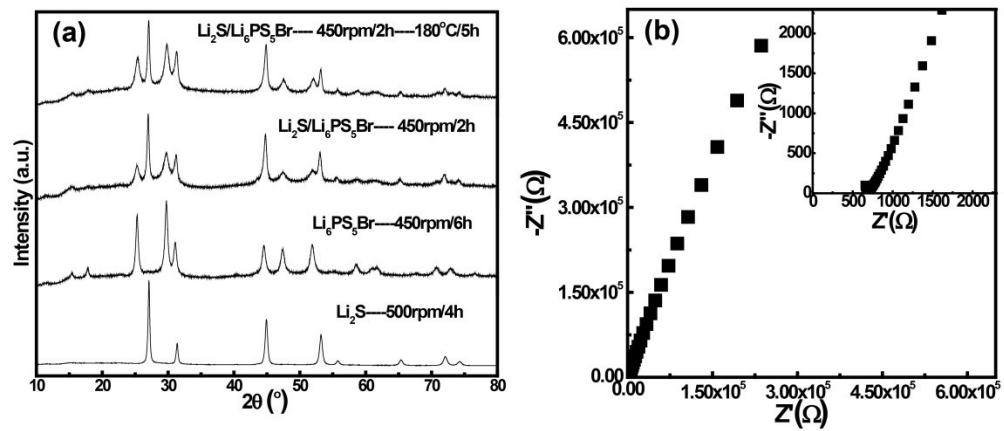


Figure S4. (a) XRD patterns of Li_2S cathode, $\text{Li}_6\text{PS}_5\text{Br}$ electrolyte and the mixture of those two. (b) The complex impedance plot for the mixture of Li_2S and $\text{Li}_6\text{PS}_5\text{Br}$ ball milled with 450 rpm for 2 h.

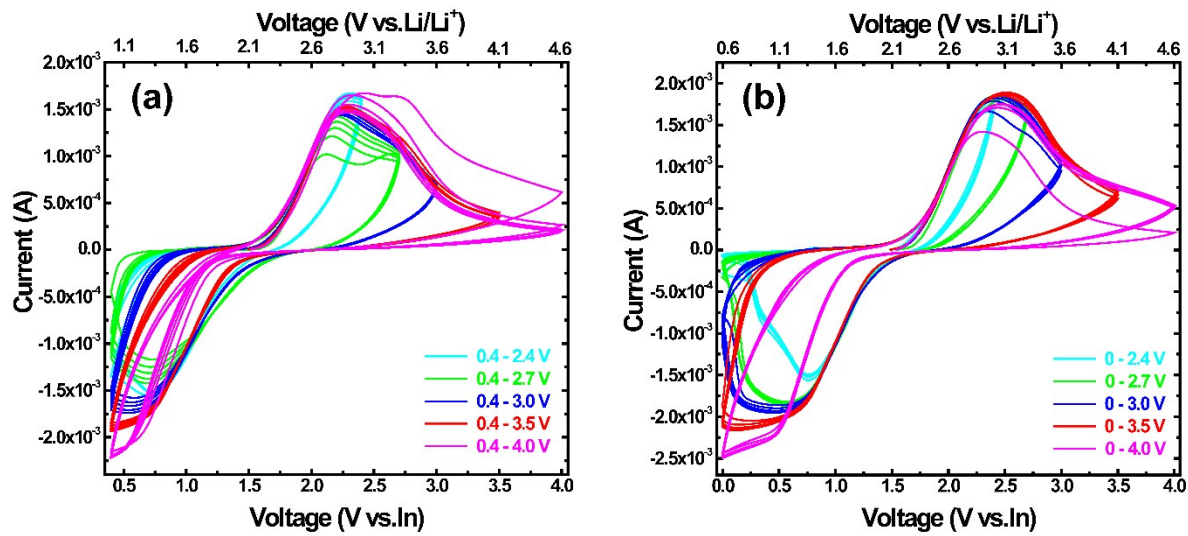


Figure S5. Cyclic voltammograms of the nano-Li₂S/AN-Li₆PS₅Br/Li-In all-solid-state batteries for different voltage cut-off windows (a) 0.4 - 2.4, 0.4 - 2.7, 0.4 - 3.0, 0.4 - 3.5, and 0.4 to 4.0 V and (b) 0 - 2.4, 0 - 2.7, 0 - 3.0, 0 - 3.5, and 0 - 4.0 V; all vs. In, at a scanning rate of 0.5 mV/s. The bottom X-axis shows the values of the voltage versus In, the top X-axis shows the corresponding values of voltage versus Li/Li⁺.